Enhancement of Spin Lifetime in Gate-Fitted InGaAs Narrow Wires

Yoji Kunihashi,[1] Makoto Kohda,[1,2] and Junsaku Nitta[1]

[1]Department of Materials Science, Tohoku University, Aramaki-Aza Aoba, Aoba-ku, Sendai 980-8579, Japan
[2]PRESTO, Japan Science and Technology Agency, Kawaguchi, Saitama 332-0012, Japan

(Received 5 December 2008; published 2 June 2009)

We investigated the spin lifetime in gate-fitted InGaAs narrow wires from magnetotransport measurement. Applying positive gate bias voltage, the spin lifetimes in narrow wires became more than one order longer than those obtained from a Hall bar sample with two-dimensional electron gas. This enhancement of spin lifetime in gated wires is the first experimental evidence of dimensional confinement and resonant spin-orbit interaction effect controlled by gate bias voltage. Spin relaxation due to the cubic Dresselhaus term is negligible in the present InGaAs wires.

DOI: 10.1103/PhysRevLett.102.226601 PACS numbers: 72.25.Rb, 73.20.Fz, 73.21.Hb, 73.61.Ey

In addition to the charge of electrons, spin degree of freedom in semiconductors is a promising candidate for controllable information carriers in novel spintronics devices [1–3] and quantum computing [4]. Both electrical spin manipulation and long spin lifetime are significantly important for such spin-based information devices. A spin-orbit interaction (SOI) gives rise to an effective magnetic field, which induces spin precession of moving electrons. Since the potential gradient in two-dimensional electron gas (2DEG) can be controlled by external gate bias, the Rashba SOI [5] enables spin manipulation by electrical means [6,7]. However, an SOI is a double-edged sword because its momentum-dependent effective magnetic field randomizes spin orientations due to the D'yakonov-Perel' (DP) spin relaxation mechanism [8].

Recently, much attention is being focused on the suppression of spin relaxation in the presence of SOIs. One way to suppress spin relaxation is dimensional confinement of the momentum of electrons with a narrow channel whose width W is less than the bulk spin precession length L_{SO} [9]. This dimensional confinement effect has been confirmed by transport measurement using weak antilocalization (WAL) analysis [10–12] and by optical measurement [13]. Since the confinement effect can be controlled by the gate modulation of $L_{SO} = \hbar^2/2\alpha m_e$ via the Rashba SOI parameter α, electrical control of spin relaxation is also possible in narrow wires. However, this electrical control of spin relaxation has not yet been experimentally confirmed by using gate-fitted narrow wires.

Another way to suppress spin relaxation is the utilization of a uniaxially oriented effective magnetic field where the linear Dresselhaus SOI [14] parameter β is equal to α [15–17], when the cubic Dresselhaus parameter γ is negligibly small. This uniaxial effective magnetic field yields persistent spin helix (PSH) state in which the DP mechanism is completely suppressed, leading to infinite spin lifetime [2]. After this theoretical prediction, PSH has recently been reported in optical spin lifetime measurement by using the transient spin-grating technique [17]. Since demonstration of resonant SOI effect with gate modulation is of importance for future spintronics devices, electrical manipulation of α in narrow wires has great potential for both electrical spin manipulation and long spin lifetime.

In this Letter, we investigated gate voltage dependence of magnetoconductance in InGaAs-based narrow wires. We found that the spin lifetime in narrow wires becomes more than one order longer than that in a Hall bar in the higher carrier density region. This remarkable increase of spin lifetime can be attributed to the effect of uniaxial effective magnetic fields due to $\alpha \to \beta$ as well as to the dimensional confinement in narrow wires.

The epitaxial $In_{0.52}Al_{0.48}As/In_{0.53}Ga_{0.47}As/In_{0.7}Ga_{0.3}As$ (quantum well) $/In_{0.53}Ga_{0.47}As/InP$ heterostructure grown on (001) InP was processed into sets of wires which were aligned along $[1\bar{1}0]$ using electron beam lithography and reactive ion etching as shown in Fig. 1(a). Each sample consisted of 95 identical 650-μm-long wires covered by SiO_2/AuGeNi gate electrode. Geometrical width W_{SEM} of the wire defined by scanning electron microscopy were 477, 566, 766, 861, 1026, and 1263 nm. Gate voltage dependences of carrier density N_s and mobility μ for a Hall bar and each wire structures were determined from sheet resistance and the fast Fourier transformation of Shubnikov–de Haas oscillation at $T = 0.3$ K. The observed WAL in the Hall bar was fitted by the Iordanskii, Lyanda-Geller, and Pikus (ILP) model [18] to extract the gate voltage dependence of α as shown in Fig. 1(b) and bulk spin precession length $L_{SO} = \hbar^2/2\alpha m_e$. This carrier density dependence of α is consistent with α calculated by the $k \cdot p$ formalism [19].

We now turn to the transport properties in narrow wires. As shown in Fig. 1(c), conductance of different narrow wires with no gate bias in the absence of a magnetic field show linear width dependence. Depletion width $W_{dep} = 309$ nm is deduced from the x-intercept. It turns out that electron motion in wires is limited by effective width $W_{eff} = W_{SEM}$-W_{dep} rather than by W_{SEM}. Magnetoconductance data are shown in Fig. 1(d). Crossover from WAL to weak localization (WL) is observed with the reduction of W_{SEM}. This width dependence

 © 2009 The American Physical Society

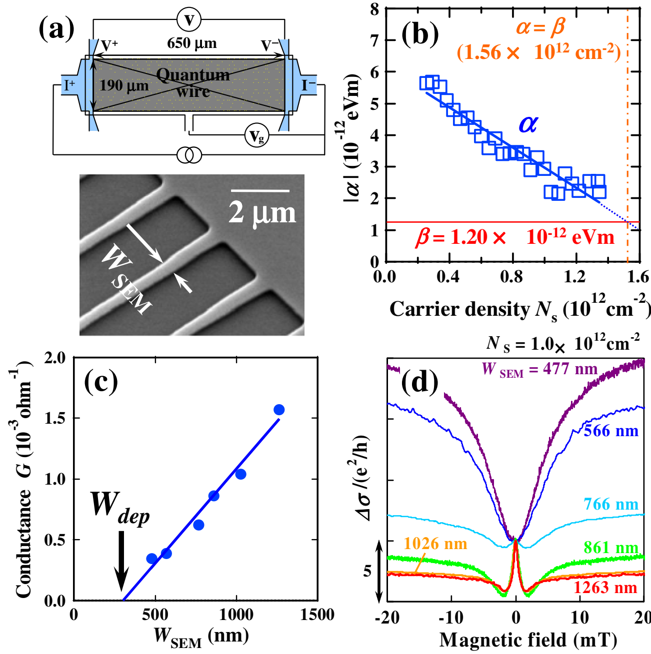

FIG. 1 (color online). (a) Schematic illustration and scanning electron micrograph of narrow wire structure. (b) Carrier density dependence of Rashba parameter α by fitting ILP model to magmetoconductance of Hall bar structure. Solid line is derived by the least-square method. (c) W_{SEM} dependence of conductance G. Solid line is derived by the least-square method and its x-intercept means depletion width W_{dep}. (d) Magnetoconductance with different wire widths W_{SEM} in units of e^2/h. All curves were measured at $N_s = 1.0 \times 10^{12}$ cm^{-2}, $T = 0.3$ K.

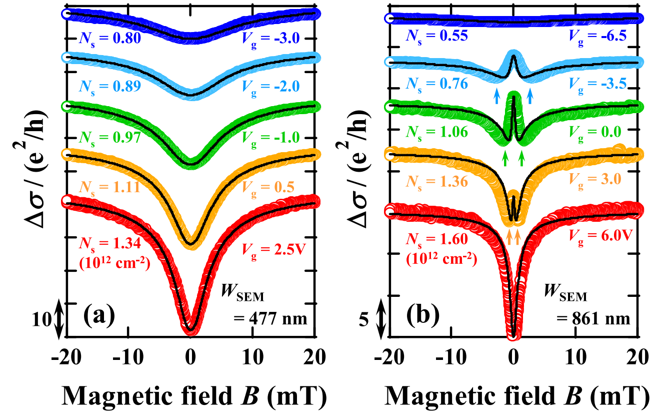

FIG. 2 (color online). Magnetoconductance with different gate bias voltages in units of $e^2/h(W_{\mathrm{SEM}} = 477$ and 861 nm). Solid lines show the fitting results of Kettemann model.

of magnetoconductance indicates that spin relaxation is suppressed by decreasing the wire width as reported by Schäpers *et al.* [10]. We then measured the gate voltage dependence of magnetoconductance with different wire widths. The experimental results for the wire of $W_{\mathrm{SEM}} =$ 477 and 861 nm are shown in Fig. 2. Narrow wires with $W_{\mathrm{SEM}} = 477$ and 566 nm showed only WL through out the entire gate region. This implies that spin relaxation length $l_{\mathrm{SO}}^{\mathrm{1D}}$ in such narrow wires is always longer than the inelastic scattering length l_ϕ which increases with carrier densities. In contrast, in the cases of the wires whose widths are $W_{\mathrm{SEM}} = 766$ and 861 nm, twofold crossover of WL-WAL-WL was observed when the carrier densities were increased.

In the case of narrow wire in which l_ϕ exceeds W_{eff}, the ILP model is no longer applicable. Recently, Kettemann has developed a model describing quantum correction of conductivity with lateral confinement and SOIs effect [20]. First, we deduced carrier density dependence of W_{dep} from the fitting of the Kettemann model to the magnetoconductance observed for 477 nm wire with fitting parameter l_ϕ and W_{eff} following previous study [21], and we confirmed that $W_{\mathrm{dep}} = 313 \pm 15$ nm is almost constant with carrier density. We then fitted the Kettemann model to the experimental results with the fitting parameters of $l_{\mathrm{SO}}^{\mathrm{1D}}$ and l_ϕ, in which W_{dep} is fixed at 313 nm. Indeed, not all of our experimental data in the wider wire than $W_{\mathrm{SEM}} =$ 766 nm are included in the applicable region of the Kettemann model, i.e., $W_{\mathrm{eff}} < L_{\mathrm{SO}}$. Nevertheless, even in the case of 1263-nm wide narrow wire, we confirmed that magnetic field at the conductance minima corresponding to the spin relaxation magnetic field $H_{\mathrm{SO}} = 1.3$ mT is much smaller than $H_{\mathrm{SO}} = 3.2$ mT of Hall bar. This decrease of H_{SO} strongly indicates that dimensional confinement effect already appears in the wire of $W_{\mathrm{SEM}} = 1263$ nm although $W_{\mathrm{eff}} = 950$ nm is 3 times longer than $L_{\mathrm{SO}} = 314$ nm at $N_s = 1.0 \times 10^{12}$ cm^{-2}. Thus, we applied the Kettemann model to the magnetoconductance data over the range of $W_{\mathrm{eff}} < L_{\mathrm{SO}}$. Extracted $l_{\mathrm{SO}}^{\mathrm{1D}}$ and l_ϕ are plotted in Fig. 3 with l_{el}, elastic scattering length. For all wires, l_ϕ and l_{el} monotonously increase with increasing N_s. In the cases of $W_{\mathrm{SEM}} = 766$ and 861 nm, $l_{\mathrm{SO}}^{\mathrm{1D}}$ shows rapid increase in the high carrier density region above 1.4×10^{12} cm^{-2}. From Figs. 3(c) and 3(d), suppression of WAL in the low carrier density region is seen to be caused by the decrease of l_ϕ. The reduction of l_ϕ with negative gate voltages can be explained in terms of the electron-electron scattering rate due to decreasing carrier density and mobility [22]. On the other hand, suppression of WAL in the high carrier density region is caused by the rapid increase of $l_{\mathrm{SO}}^{\mathrm{1D}}$, which exceeds l_ϕ.

Even though the Ketteman model is only available for the diffusive wires, we confirmed that the Kettemann model is applicable for the wire investigated here by comparing the quantum correction in one-dimensional limit (ballistic regime) without SOI developed by Beenakker and van Houten (BvH) [23]. In narrow wires of $W_{\mathrm{SEM}} = 477$ and 566 nm, we observed WL in whole gate voltage region. Therefore, the phase coherent length obtained by the Ketteman model $l_{\mathrm{SO}}^{\mathrm{1D}} = l_\varphi$ can be compared with these obtained by the BvH model as shown filled and open squares, respectively, in Figs. 3(a) and 3(b). We found that both two models provide more or less

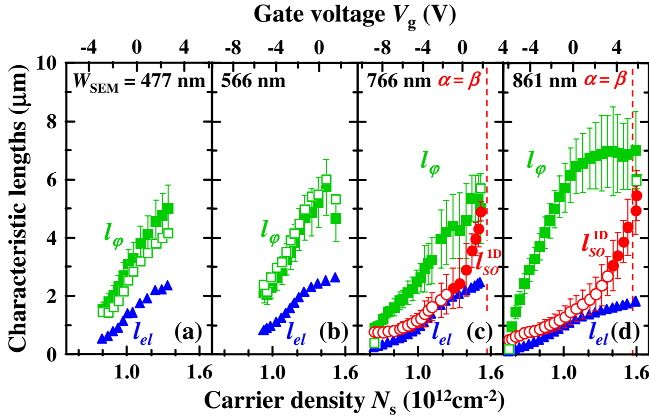

FIG. 3 (color online). Carrier density dependence of the characteristic lengths. l_φ, $l_{\rm SO}^{\rm 1D}$ and l_{el} correspond to phase coherent length (closed and open squares), spin relaxation length in one-dimensional system (closed and open circles), and elastic scattering length (closed triangles), respectively. Open circles indicate the $l_{\rm SO}^{\rm 1D}$ which were obtained in the outside of the applicable region, $W_{\rm eff} < L_{\rm SO}$, of Kettemann model. Closed and open squares indicate l_ϕ obtained by fitting Kettemann model and BvH model to the WL data, respectively. Dashed lines indicate specified $N_s = 1.56 \times 10^{12}$ cm^{-2}, where $\alpha = \beta$ is expected.

similar values of phase coherent lengths showing the validity of the Ketteman model for the ballistic wire investigated here. Same conclusions are also found in Figs. 3(c) and 3(d).

To understand this enhancement of $l_{\rm SO}^{\rm 1D}$ in the high carrier density region, we considered the spin relaxation rate in the quasi one-dimensional structure derived by Kettemann [20]:

$$\frac{1}{\tau_{\rm SO}^{\rm 1D}} = \frac{1}{12}\left(\frac{W_{\rm eff}}{L_{\rm SO}}\right)^2 \delta_{\rm SO}^2 \frac{1}{\tau_{\rm SO}^{\rm 2D}} + D\frac{(m_e^2 E_F \gamma/\hbar^2)^2}{\hbar^4}, \quad (1)$$

where D, m_e, and E_F are diffusion constant, effective mass of an electron, and Fermi energy, respectively. $\delta_{\rm SO}$ is given by

$$\delta_{\rm SO} = (Q_R^2 - Q_D^2)/(Q_R^2 + Q_D^2), \qquad Q_R = 2m_e\alpha/\hbar^2,$$
$$Q_D = m_e(2\beta - m_e E_F \gamma/\hbar^2)/\hbar^2.$$

The first term in Eq. (1) is the modified spin relaxation rate from 2DEG $\tau_{\rm SO}^{\rm 2D}$ due to the dimensional confinement, $(W_{\rm eff}/L_{\rm SO})^2$, and the resonant SOI effect, $\delta_{\rm SO}$. The second term in Eq. (1) shows the spin relaxation rate induced by the cubic Dresselhaus term. As shown in Fig. 4, enhancement of $l_{\rm SO}^{\rm 1D} = \sqrt{D\tau_{\rm SO}^{\rm 1D}}$ due to dimensional confinement is confirmed at various carrier densities. However, $l_{\rm SO}^{\rm 1D}$ calculated from Eq. (1) are much smaller than experimental results as shown by dashed lines, especially in the high carrier density and the small width region, due to spin relaxation rate based on the second term of Eq. (1). Thus, we calculated $l_{\rm SO}^{\rm 1D}$ neglecting second term in Eq. (1). The recalculated $l_{\rm SO}^{\rm 1D}$, shown as solid lines in Fig. 4, show good agreements with experimental data. From this analysis, it is found that spin relaxation due to the cubic Dresselhaus term may be suppressed by dimensional confinement in the present sample. When we consider pure 1D wires under the existence of cubic Dresselhaus SOI, DP spin relaxation is completely suppressed since the effective magnetic field only changes its sign due to 1D electron motion. Thus, it may be natural to reach the suppression of the cubic Dresselhaus SOI as the wire goes to ballistic limit. We then plotted the spin lifetimes $\tau_{\rm SO}^{\rm 1D}$ as a function of the dimensional confinement parameter $(L_{\rm SO}/W_{\rm eff})^2$ in Fig. 5.

In Fig. 5, spin lifetime $\tau_{\rm SO}^{\rm 1D}$ observed in 766- and 861-nm-wide wires rapidly increases when dimensional confinement becomes much stronger, i.e., $(L_{\rm SO}/W_{\rm eff})^2 > 1$. To understand the enhancement of spin lifetime, $\tau_{\rm SO}^{\rm 1D}$ in Eq. (1), where all SOI contributions are taken into account, was calculated as shown by the green dashed-dotted line in Fig. 5 with $\beta = 1.20 \times 10^{-12}$ eVm estimated from $\beta = \gamma\langle k_z^2\rangle$, where the parameter of cubic Dresselhaus term $\gamma = 2.73 \times 10^{-29}$ eVm^3 [24] and wave number along the quantized direction $k_z = 2\pi/\lambda$. Here, λ is the electron wave length inside the QW. The calculated spin lifetime dose not increase and remains very small with the increase of $(L_{\rm SO}/W_{\rm eff})^2$. As a result, we cannot explain the rapid increase of spin lifetime if all SOI contributions are taken into account. In contrast, $\tau_{\rm SO}^{\rm 1D}$ with neglecting second term in Eq. (1) rapidly increases with the increase of $(L_{\rm SO}/W_{\rm eff})^2$ and shows good agreement with the experimental results for wires of both $W_{\rm SEM} = 766$ and 861 nm. In addition, as shown by the dashed lines in Fig. 5, when the resonant SOI effect is neglected, i.e., $\delta_{\rm SO} = 1$, enhancement of spin lifetime is limited with increasing $(L_{\rm SO}/W_{\rm eff})^2$ in contrast to the solid line taking both the resonant SOI effect and the dimensional confinement into

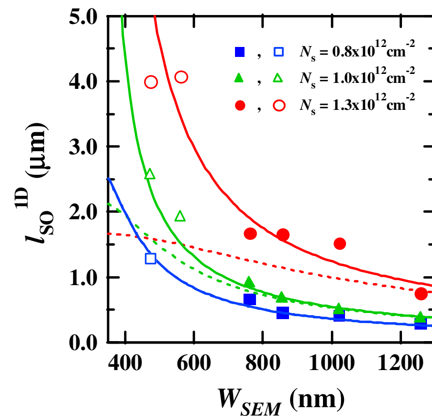

FIG. 4 (color online). Width dependence of $l_{\rm SO}^{\rm 1D}$ of different carrier density. Solid lines and dashed lines show the $l_{\rm SO}^{\rm 1D}$ calculated from Eq. (1) with neglecting second term and taking into account full SOIs, respectively. At $N_s = 0.8 \times 10^{12}$ cm^{-2}, dashed line is on top of solid line, meaning the second term is negligible. Open symbols show the l_ϕ obtained by fitting Kettemann model to the WL data which corresponds to minimum values of $l_{\rm SO}^{\rm 1D}$.

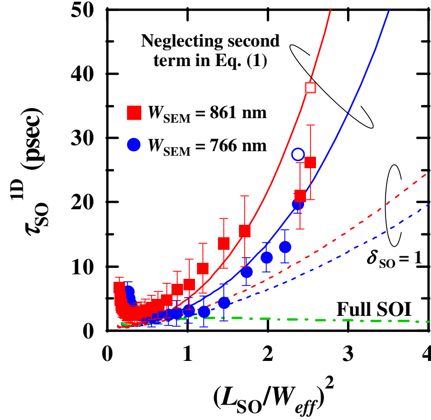

FIG. 5 (color online). Spin lifetime obtained by the Kettemann model as a function of dimensional confinement $(L_{SO}/W_{eff})^2$. Dashed and dashed-dotted lines show spin lifetime calculated by Eq. (1) by neglecting the resonant SOI effect where $\delta_{SO} = 1$ and by taking all SOI contributions into account, respectively. Solid lines are calculated with second term of Eq. (1) neglected. Open symbols show inelastic scattering time τ_ϕ extracted from the fitting by BvH model.

account. According to Fig. 1(b), resonant SOI effect is expected at $N_s = 1.56 \times 10^{12}$ cm^{-2} since estimated linear Dresselhaus SOI parameter β is 1.20×10^{-12} eVm. This carrier density corresponds to the enhancement of spin relaxation length observed in the wire of $W_{SEM} = 766$ and 861 nm in Figs. 3(c) and 3(d). Consequently, the dominant contribution of the enhanced spin lifetime is for approaching both the resonant SOI condition where the effective magnetic field is uniaxial and the dimensional confinement due to the electrical modulation of $(L_{SO}/W_{eff})^2$. The above data analysis suggests that the spin relaxation due to the cubic Dresselhaus term is also suppressed by the geometrical confinement effect.

On the contrary, Holleitner *et al.* have observed saturation of spin lifetime with decreasing wire width [13]. They have attributed this saturation to the cubic Dresselhaus SOI or Elliot-Yafet spin relaxation mechanism. We did not observe cubic Dresselhaus effect in the present wire samples. This discrepancy is an open question and it will be for future study.

Furthermore, to confirm the enhanced spin lifetime, we also fitted WL data observed at maximum $(L_{SO}/W_{eff})^2$ by BvH model. Since the τ_ϕ derived by BvH corresponds to the lower limit of spin lifetime, we can estimate the minimum value of τ_{SO}^{1D}. Inelastic scattering time $\tau_\phi = 27.4$ and 37.8 psec were extracted by fitting of the BvH model for wires of $W_{SEM} = 766$ and 861 nm, respectively. Extracted τ_ϕ are shown as open symbols in Fig. 5, which show similar values of the spin lifetime derived from the Kettemann model. Consequently, enhanced spin lifetime was again confirmed by different theoretical approaches.

In conclusion, gate voltage dependence of magnetoconductance in InGaAs narrow wires was investigated. In wire widths of $W_{SEM} = 766$ and 861 nm, twofold crossover of WL-WAL-WL was observed by changing gate bias voltage. From the comparison between experimental data and theoretical model, it was found that spin lifetime is enhanced one order longer than in the case of the Hall bar in the high carrier density region. This remarkable enhancement of spin lifetime was explained by considering both dimensional confinement and resonant SOI effect. Surprisingly, our experimental results suggest that the spin relaxation due to the cubic Dresselhaus term is also suppressed in the present InGaAs wires. A gate-fitted InGaAs wire enables electrical manipulation together with long spin lifetime.

The authors wish to thank S. Kettemann and M. Scheid for valuable discussions. This work was partly supported by Grants-in-Aid from JSPS, MEXT, and SCOPE of the Ministry of Internal Affairs and Communications. This work was partly carried out at the Laboratory for Nanoelectronics and Spintronics, Research Institute of Electrical Communication, Tohoku University.

[1] S. Datta and B. Das, Appl. Phys. Lett. **56**, 665 (1990).
[2] X. Cartoxiá, D. Z. -Y. Ting, and Y.-C. Chang, Appl. Phys. Lett. **83**, 1462 (2003).
[3] M. Ohno and K. Yoh, Phys. Rev. B **77**, 045323 (2008).
[4] D. D. Awschalom, D. Loss, and N. Samarth, *Semiconductor Spintronics and Quantum Computation* (Springer, New York, 2002).
[5] E. I. Rashba, Sov. Phys. Solid State **2**, 1109 (1960).
[6] J. Nitta *et al.*, Phys. Rev. Lett. **78**, 1335 (1997).
[7] T. Bergsten *et al.*, Phys. Rev. Lett. **97**, 196803 (2006).
[8] M. I. D'yakonov and V. I. Perel', Sov. Phys. Solid State **13**, 3023 (1971).
[9] A. Bournel *et al.*, Eur. Phys. J. Appl. Phys. **4**, 1 (1998); A. G. Mal'shukov and K. A. Chao, Phys. Rev. B **61**, R2413 (2000); A. A. Kiselev and K. W. Kim, Phys. Rev. B **61**, 13 115 (2000); T. P. Pareek and P. Bruno, Phys. Rev. B **65**, 241305(R) (2002).
[10] Th. Schäpers *et al.*, Phys. Rev. B **74**, 081301(R) (2006).
[11] A. Wirthmann *et al.*, Physica (Amsterdam) **34E**, 493 (2006).
[12] P. Lehnen *et al.*, Phys. Rev. B **76**, 205307 (2007).
[13] A. W. Holleitner *et al.*, Phys. Rev. Lett. **97**, 036805 (2006).
[14] G. Dresselhaus, Phys. Rev. **100**, 580 (1955).
[15] J. Schliemann and D. Loss, Phys. Rev. B **68**, 165311 (2003).
[16] B. Andrei Bernevig, J. Orenstein, and Shou-Cheng Zhang, Phys. Rev. Lett. **97**, 236601 (2006).
[17] D. Koralek *et al.*, Nature (London) **458**, 610 (2009).
[18] S. V. Iordanskii, Y. B. Lyanda-Geller, and G. E. Pikus, JETP Lett. **60**, 206 (1994).
[19] Th. Schäpers *et al.*, J. Appl. Phys. **83**, 4324 (1998).
[20] S. Kettemann, Phys. Rev. Lett. **98**, 176808 (2007).
[21] S. J. Koester *et al.*, Phys. Rev. B **54**, 10 604 (1996).
[22] J. A. Katine *et al.*, Phys. Rev. B **57**, 1698 (1998).
[23] C. W. J. Beenakker and H. van Houten, Phys. Rev. B **38**, 3232 (1988).
[24] R. Winkler, *Spin-Orbit Coupling Effects in Two-Dimensional Electron and Hole Systems* (Springer, New York, 2003).